

INCLUDING PIONS^a ^b

Martin J. Savage ^c

Department of Physics, University of Washington, Seattle, WA 98195

Recent progress in using effective field theory to describe systems with two nucleons is discussed with particular emphasis placed on the inclusion of pions. Inconsistencies arising in Weinberg's power counting are demonstrated with two concrete examples. A consistent power-counting scheme is discussed in which pion exchange is sub-leading to local four-nucleon operators. NN scattering in the 1S_0 and $^3S_1 - ^3D_1$ channels is calculated at sub-leading order and compared with data.

1 Introduction

The last several years have seen significant progress towards an effective field theory description of the interactions between nucleons. The ultimate goal of this endeavour is to construct a framework with which to describe multi-nucleon systems, both bound and unbound, and inelastic processes in a systematic way. This effort was initiated by Weinberg's pioneering work on the subject¹ where he proposed a power-counting scheme for local-operators involving two or more nucleons and the inclusion of pions. This proposal had many important implications from detailing how to include higher order terms in the chiral and derivative expansion to the prediction of small three-body forces. Applications to phenomenology, such as studies of the NN phase-shifts, $np \rightarrow D\gamma$ radiative capture, nucleon-deuteron scattering, as well as extensive discussion of the underlying field theory itself have followed Weinberg's original proposal²⁻¹⁹. Problems with Weinberg's power-counting became apparent when computations were performed with dimensional regularization⁴, as opposed to a momentum-space regulator that previous computations had employed². Contributions to NN scattering in the $^3S_1 - ^3D_1$ channel that are leading order in Weinberg's power-counting require counterterms at all orders in the momentum expansion, and therefore terms that are naively subleading order must be included at leading order. One is lead to the conclusion that Weinberg's power-counting is not consistent.

Recently, a new and consistent power-counting scheme has been proposed¹⁷ that alleviates the difficulties encountered with Weinberg's power-counting. It is this power-counting and its implications that I will present with an em-

^aTalk presented at the Joint Caltech/INT workshop on **Nuclear Physics with Effective Field Theory**, Caltech, February 1998.

^bNT@UW-11

^cWork done in collaboration with David B. Kaplan and Mark B. Wise

phasis on the theory with pions. Firstly, I will discuss Weinberg's power-counting scheme and its shortcomings. Next, I will discuss a new power-counting scheme¹⁷ and show results from its application to NN scattering in the 1S_0 and $^3S_1 - ^3D_1$ channels at subleading order.

2 Weinberg's Power Counting

Effective field theories (EFT) are constructed to reproduce all S-matrix elements with external momenta $\sim Q$ less than some scale Λ . The scale Λ is typically set by the mass of particles and kinematic regimes not explicitly included in the theory as dynamical degrees of freedom. However, the effect of these particles and regimes are included in the EFT by the presence of higher dimension operators, with coefficients explicitly set by Λ . In addition to forming the lagrange density consistent with the global and local symmetries of the underlying theory, one must also define the method of regulating divergences. It is desirable to choose a regulator that preserves the symmetries of the theory and also maintains the hierarchy of the higher dimension operators. Here we reproduce Weinberg's power-counting scheme^{1,4}, without an explicit discussion of the method of regularization, therefore the conclusions are regulator independent.

The most general lagrange density consistent with chiral symmetry describing the interaction of two nucleons is

$$\begin{aligned} \mathcal{L} = & N^\dagger (iD_0 + \vec{D}^2/2M)N + \frac{f^2}{8} \text{Tr} \partial_\mu \Sigma^\dagger \partial^\mu \Sigma + \frac{f^2}{4} \omega \text{Tr} m_q (\Sigma + \Sigma^\dagger) \\ & - \frac{1}{2} C_S (N^\dagger N)^2 - \frac{1}{2} C_T (N^\dagger \vec{\sigma} N)^2 + g_A N^\dagger \vec{A} \cdot \vec{\sigma} N + \dots , \end{aligned} \quad (1)$$

where D_μ denotes a chiral-covariant derivative and Σ is the exponential of the isovector triplet of pions

$$\begin{aligned} \Sigma &= \exp \left(\frac{2i}{f} M \right) \\ M &= \begin{pmatrix} \pi^0/\sqrt{2} & \pi^+ \\ \pi^- & -\pi^0/\sqrt{2} \end{pmatrix} , \end{aligned} \quad (2)$$

with $f = 132$ MeV the pion decay constant and \vec{A} is the axialvector meson field. The ellipses denote terms with more spatial derivatives and also more insertions of the light quark mass matrix, m_q . The Georgi-Manohar²⁰ naive dimensional analysis arising from a consideration of loop contributions to observables suggests that $C_{S,T} \sim 1/f^2$, and Weinberg's power-counting will follow directly.

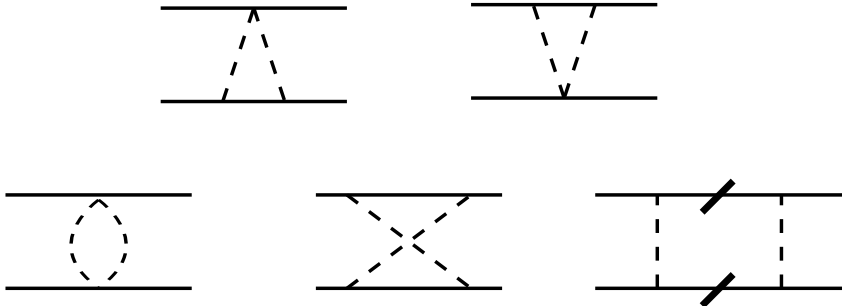


Figure 1: 2-pion exchange Feynman graphs contributing to the 2-nucleon potential $V^{(2)}$. The first four are 2-nucleon irreducible; the last diagram is 2-nucleon reducible, and the poles from the slashed propagators are not included in the $\int dq_0$ loop integration.

A necessary ingredient for an EFT is a power counting scheme that dictates which graphs to compute in order to determine an observable to a desired order in the expansion. The main complication in the theory of nucleons and pions is the fact that a nucleon propagator $S(q) = i/(q_0 - \mathbf{q}^2/2M)$ scales like $1/Q$ if q_0 scales like m_π or an external 3-momentum, while $S(q) \sim M/Q^2$ if q_0 scales like an external kinetic energy. Similarly, in loops $\int dq_0$ can scale like Q or Q^2/M , depending on which pole is picked up. To distinguish between these two scaling properties it is convenient to define generalized “ n -nucleon potentials” $V^{(n)}$ comprised of those parts of connected Feynman diagrams with $2n$ external nucleon lines that have no powers of M in their scaling (except from relativistic corrections). Since there is no nucleon-antinucleon pair creation in the effective theory such a diagram always has exactly n nucleon lines running through it. $V^{(n)}$ includes diagrams which are n -nucleon irreducible and parts of diagrams which are 1-nucleon irreducible. To compute the latter contribution to $V^{(n)}$ one identifies all combinations of two or more internal nucleon lines that can be simultaneously on-shell, and excludes their pole contributions when performing the $\int dq_0$ loop integrations. An example of the 2-pion exchange contributions to $V^{(2)}$ is shown in Fig.(1). A general n -nucleon Feynman diagram in the EFT can be constructed by contracting the nucleon legs of $V^{(r)}$ potentials with $r \leq n$. Treating the $V^{(r)}$ ’s like vertices, the $\int dq_0$ loop integrations pick up the poles of all the connecting nucleon lines. The reason for this construction is that within the $V^{(r)}$ potentials, all nucleon propagators are off-shell and scale like $1/q_0 \sim 1/Q$. In contrast, when one picks up the pole contribution from

one of the nucleon lines connecting the $V^{(r)}$ “vertices”, other nucleon lines will be almost on-shell, and scale like M/Q^2 . A contribution to the r -nucleon potential $V^{(r)}$ with ℓ loops, I_n nucleon propagators, I_π pion propagators, and V_i vertices involving n_i nucleon lines and d_i derivatives, scales like Q^μ , where

$$\begin{aligned}\mu &= 4\ell - I_n - 2I_\pi + \sum V_i d_i \quad , \\ \ell &= I_n + I_\pi - \sum V_i + 1 \quad , \\ I_n + r &= \frac{1}{2} \sum V_i n_i \quad .\end{aligned}\tag{3}$$

In this power counting we take $m_\pi \sim Q$ and treat factors of the u and d quark masses at the vertices as order Q^2 . Combining these relations leads to the scaling law for the r -nucleon potential $V^{(r)}$ ($r \geq 2$):

$$\mu = 2 + 2\ell - r + \sum_i V_i (d_i + \frac{1}{2} n_i - 2) \quad .\tag{4}$$

Since chiral symmetry implies that the pion is derivatively coupled, it follows that $(d_i + \frac{1}{2} n_i - 2) \geq 0$, which implies that for a 2-nucleon potential, $\mu \geq 0$, and that $\mu = 0$ corresponds to tree diagrams. It is straight forward to find the scaling property for a general Feynman amplitude, by repeating the analysis that leads eq.(4) treating the $V^{(r)}$ potentials as r -nucleon vertices with μ derivatives, μ given by eq.(4). While eq.(4) was derived assuming that $\int dq_0 \sim Q$ and nucleon propagators scaled like $\sim 1/Q$, for these loop graphs they scale like Q^2/M and M/Q^2 respectively. A general Feynman diagram is constructed by stringing together r -nucleon potentials $V^{(r)}$.

Two nucleon scattering is simple since the graphs are all ladder diagrams with insertions of $V^{(2)}$ ’s acting as ladder rungs. Each loop of the ladder introduces a loop integration ($dq_0 d^3 \mathbf{q} \sim Q^5/M$) and two nucleon propagators (M^2/Q^4) to give a factor of (QM) per loop. Expanding $V^{(2)} = \sum_{\mu=0}^{\infty} V_\mu^{(2)}$, where $V_\mu^{(2)} \sim Q^\mu$, a 2-nucleon diagram whose i^{th} rung is the generalized potential $V_{\mu_i}^{(2)}$ scales as

$$Q^\nu (QM)^L \quad , \quad \nu = \sum_{i=1}^{L-1} \mu_i \quad ,\tag{5}$$

where L is the number of loops external to the $V^{(2)}$ ’s. Since $\mu_i \geq 0$, the leading behavior of the 2-nucleon amplitude is $(QM)^L$. If one treats $M \simeq Q^0$, it follows that perturbation theory is adequate for describing the 2-nucleon

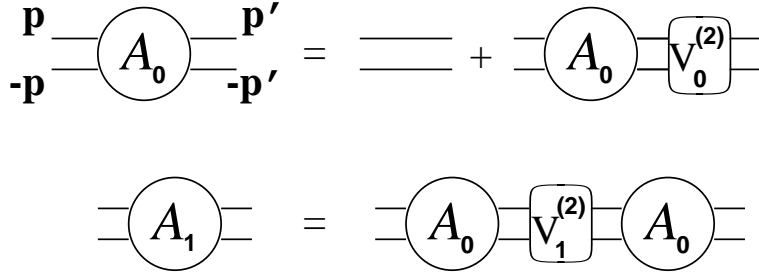


Figure 2: The first two terms in the EFT expansion of the Feynman amplitude for nucleon-nucleon scattering in Weinberg's power-counting scheme. The leading amplitude A_0 scales like Q^0 and consists of the sum of ladder diagrams with the leading ($\mu = 0$) 2-nucleon potential $V_0^{(2)}$ at every rung. The subleading amplitude A_1 scales like Q^1 .

system at low Q . In order to accommodate large scattering lengths and bound states near threshold, as in the 1S_0 and $^3S_1 - ^3D_1$ channels one must conclude that $M \sim 1/Q$ in this power counting scheme. Thus the EFT calculation must be an expansion in ν , given by eqs.(4)(5). At leading order, $\nu = 0$, one must sum up all ladder diagrams with insertions of $V_0^{(2)}$ potentials with $\mu = 0$, while at subleading order one includes one insertion of $V_1^{(2)}$ and all powers of $V_0^{(2)}$, and so forth.

At leading order in Weinberg's power-counting there are contributions to $V_0^{(2)}$ from both the local four-nucleon operators, $C_{S,T}$ and from the exchange of a single potential pion, giving a momentum space potential of

$$V_0^{(2)}(\mathbf{p}, \mathbf{p}') = C - \left(\frac{g_A^2}{2f_\pi^2} \right) \frac{(\mathbf{q} \cdot \sigma_1 \mathbf{q} \cdot \sigma_2)(\tau_1 \cdot \tau_2)}{(\mathbf{q}^2 + m_\pi^2)} , \quad (6)$$

where C denotes the combination of $C_{S,T}$ appropriate for a given spin-isospin channel. The leading order amplitude results from summing the graphs shown in Fig. (2) resulting from this potential, i.e. solving the Schrodinger equation. In the 1S_0 channel at two-loops in the ladder sum there is a logarithmic divergence in the graph shown in Fig. (3a) that must be regulated. In dimensional regularization the divergent part of this graph is

$$-\frac{1}{\epsilon} \frac{g_A^2 m_\pi^2 M^2}{128\pi^2 f_\pi^2} C^2 , \quad (7)$$

which requires a counterterm with a single insertion of the light quark mass

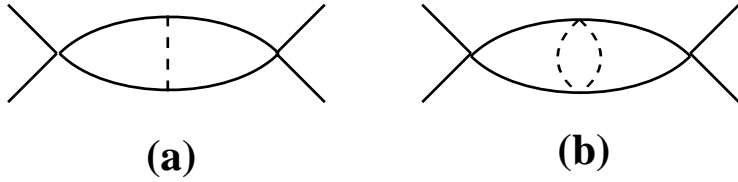


Figure 3: Graphs with logarithmic divergences. The divergence in graph (a) is proportional to $M^2 m_\pi^2$, while graph (b) has a divergence proportional to $M^2 \mathbf{p}^4$. The solid lines are nucleons and the dashed lines are pions.

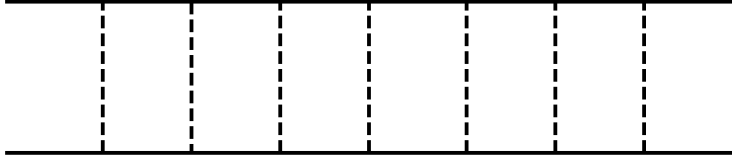


Figure 4: A contribution to the pion ladder sum, arising at leading order in Weinberg's power-counting. The solid lines are nucleons and the dashed lines are pions.

matrix, for instance

$$-\frac{1}{2} C_S^{(m)} \text{Tr} [m_q(\Sigma + \Sigma^\dagger)] (N^\dagger N)^2 - \frac{1}{2} C_T^{(m)} \text{Tr} [m_q(\Sigma + \Sigma^\dagger)] (N^\dagger \sigma N)^2 + \dots . \quad (8)$$

However, the coefficients of these operators must scale like M^2 , and since $m_\pi^2 M^2 \sim Q^0$ these formally higher order operators in Weinberg's power-counting are required at leading order to absorb divergences in the time-ordered products of the leading order potential, $V_0^{(2)}$. Ignoring the multi-pion vertices arising from these operators, they can be re-absorbed into the leading operators with coefficients $C_{S,T}$. We are then in the situation where there is no chiral expansion, multiple insertions of the light quark mass matrix are not suppressed compared to leading order interactions, but we do still have a momentum expansion in the 1S_0 channel. The graph shown in Fig. (3b) requires counterterms involving ∇^4 with coefficients proportional to M^2 , while this is not suppressed by Q^4 it is suppressed compared to the leading operators by Q^2 .

The situation is different in the $^3S_1 - ^3D_1$ channel and in higher partial waves. A contribution to the leading order ladder sum is shown in Fig. (4), arising from seven potential pion exchanges, i.e a six-loop graph. From our

discussion it is straightforward to deduce that this graph has a logarithmic divergence at order $(QM)^6$, and therefore, counterterms involving ∇^6 (i.e. operators up to and including those with orbital angular momentum $L = 6$) are required at leading order in the expansion. Clearly, the same discussion can be made for an arbitrary number of potential pion exchanges, and therefore counterterms involving an arbitrary even number of ∇ 's are required. This is a clear demonstration of the failure of Weinbergs power-counting. Further, this conclusion is true for all regularization schemes and not just for dimensional regularization. In using a momentum cut-off to regulate the theory, while truncating the expansion of the potential at a given number of derivatives one will have terms that depend explicitly upon the cut-off Λ . If the cut-off is kept small, then such terms do not have a large impact upon the “goodness of fit” to data and Λ can be chosen to achieve the “best fit”^{2,11}. The fact that the results depend upon Λ demonstrates the presence of an incomplete set of higher order terms.

As we will see in subsequent sections, the problem with Weinberg's power-counting is having to identify $M \sim Q^{-1}$ and $C \sim Q^0$. In fact consistent power-counting is obtained when we identify $M \sim Q^0$ and $C \sim Q^{-1}$.

3 A New Power Counting

Lets us begin by examining the general form of the amplitude for nucleon scattering in a S-wave

$$\mathcal{A} = \frac{4\pi}{M} \frac{1}{p \cot \delta - ip} . \quad (9)$$

From quantum mechanics it is well known that $p \cot \delta$ has a momentum expansion for $p \ll \Lambda$ (the effective range expansion),

$$p \cot \delta = -\frac{1}{a} + \frac{1}{2} \Lambda^2 \sum_{n=0}^{\infty} r_n \left(\frac{p^2}{\Lambda^2} \right)^{n+1} , \quad (10)$$

where a is the scattering length, and r_0 is the effective range. For scattering in the 1S_0 and 3S_1 channels the scattering lengths are found to be large, $a^{(^1S_0)} = -23.714 \pm 0.013$ fm and $a^{(^3S_1)} = +5.425 \pm 0.0014$ fm respectively. Expanding the expression for the amplitude in eq.(9) in powers of p/Λ while retaining ap to all orders gives

$$\mathcal{A} = -\frac{4\pi}{M} \frac{1}{(1/a + ip)} \left[1 + \frac{r_0/2}{(1/a + ip)} p^2 + \frac{(r_0/2)^2}{(1/a + ip)^2} p^4 + \frac{(r_1/2\Lambda^2)}{(1/a + ip)} p^4 + \dots \right] \quad (11)$$

For $p > 1/|a|$ the terms in this expansion scale as $\{p^{-1}, p^0, p^1, \dots\}$, and the expansion in the effective theory takes the form

$$\mathcal{A} = \sum_{n=-1}^{\infty} \mathcal{A}_n \quad , \quad \mathcal{A}_n \sim p^n \quad . \quad (12)$$

In the theory without pions we can explicitly compute the s-wave amplitude in each spin channel to all orders in the momentum expansion,

$$\mathcal{A} = -\frac{\sum C_{2n} p^{2n}}{1 + M(\mu + ip)/4\pi \sum C_{2n} p^{2n}} \quad , \quad (13)$$

where C_{2n} is the coefficient of the p^{2n} term in the lagrange density. μ is the renormalization scale and we have used Power Divergence Subtraction (*PDS*)¹⁷ to define the theory. A typical loop graph that appears in the amplitude has the form

$$\begin{aligned} I_n &\equiv -i \left(\frac{\mu}{2}\right)^{4-D} \int \frac{d^D q}{(2\pi)^D} \mathbf{q}^{2n} \left(\frac{i}{\frac{E}{2} + q_0 - \frac{\mathbf{q}^2}{2M} + i\epsilon} \right) \left(\frac{i}{\frac{E}{2} - q_0 - \frac{\mathbf{q}^2}{2M} + i\epsilon} \right) \\ &= \left(\frac{\mu}{2}\right)^{4-D} \int \frac{d^{(D-1)} \mathbf{q}}{(2\pi)^{(D-1)}} \mathbf{q}^{2n} \left(\frac{1}{E - \frac{\mathbf{q}^2}{M} + i\epsilon} \right) \\ &= -M(ME)^n (-ME - i\epsilon)^{(D-3)/2} \Gamma\left(\frac{3-D}{2}\right) \frac{\left(\frac{\mu}{2}\right)^{4-D}}{(4\pi)^{(D-1)/2}} \quad , \quad (14) \end{aligned}$$

where D is the number of space-time dimensions. In the *PDS* scheme the pole at $D = 3$ is removed by adding a local counterterm to the lagrange density, giving

$$\delta I_n = -\frac{M(ME)^n \mu}{4\pi(D-3)} \quad , \quad (15)$$

so that the sum of the loop graph and counterterm in $D = 4$ dimensions is

$$I_n^{PDS} = I_n + \delta I_n = -(ME)^n \left(\frac{M}{4\pi}\right) (\mu + ip). \quad (16)$$

The amplitude \mathcal{A} is independent of the subtraction point μ and this determines the μ dependence of the coefficients, C_{2n} . In the *PDS* scheme one finds that for $\mu \gg 1/|a|$, the couplings $C_{2n}(\mu)$ scale as

$$C_{2n}(\mu) \sim \frac{4\pi}{M \Lambda^n \mu^{n+1}} \quad , \quad (17)$$

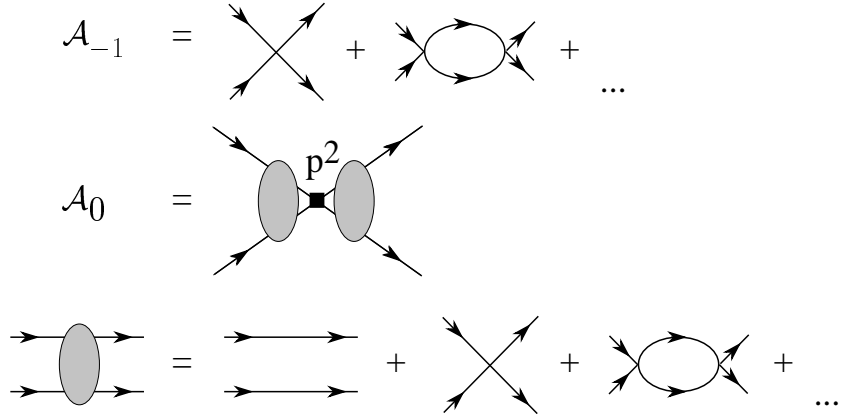


Figure 5: Leading and subleading contributions arising from local operators.

so that if we take $\mu \sim p$, $C_{2n}(\mu) \sim 1/p^{n+1}$. A factor of ∇^{2n} at a vertex scales as p^{2n} , while each loop contributes a factor of p . Therefore, the leading order contribution to the scattering amplitude \mathcal{A}_{-1} scales as p^{-1} and consists of the sum of bubble diagrams with C_0 vertices. Contributions scaling as higher powers of p come from perturbative insertions of derivative interactions, dressed to all orders by C_0 . The first two terms in the expansion

$$\mathcal{A}_{-1} = \frac{-C_0}{[1 + \frac{C_0 M}{4\pi}(\mu + ip)]} \quad , \quad \mathcal{A}_0 = \frac{-C_2 p^2}{[1 + \frac{C_0 M}{4\pi}(\mu + ip)]^2} \quad , \quad (18)$$

correspond to the Feynman diagrams in Fig. (5). A comparison with eq.(11) gives

$$C_0(\mu) = \frac{4\pi}{M} \left(\frac{1}{-\mu + 1/a} \right) \quad , \quad C_2(\mu) = \frac{4\pi}{M} \left(\frac{1}{-\mu + 1/a} \right)^2 \frac{r_0}{2} \quad . \quad (19)$$

The dependence of $C_{2n}(\mu)$ on μ is determined by requiring the amplitude be independent of the renormalization scale μ . The physical parameters a, r_n enter as boundary conditions on the resulting renormalization group (RG) equations. The beta function for each of the couplings C_{2n} is defined by

$$\beta_{2n} \equiv \mu \frac{dC_{2n}}{d\mu} \quad . \quad (20)$$

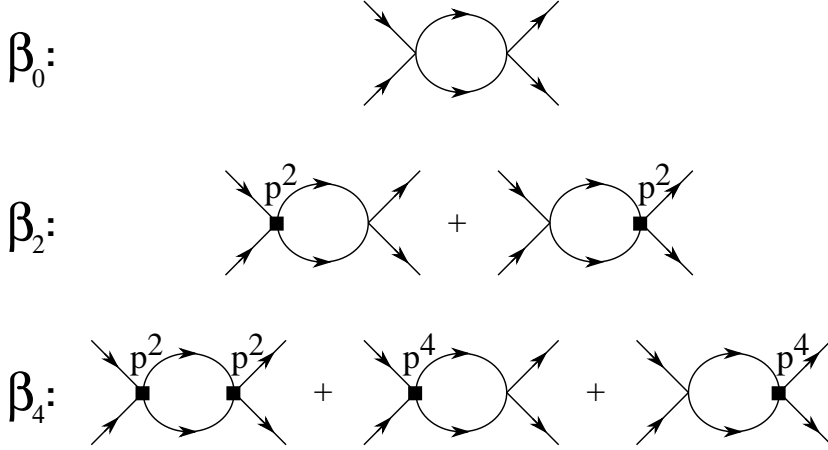


Figure 6: Graphs contributing to the β -functions for C_{2n}

In the *PDS* scheme, the μ dependence of the C_{2n} coefficients enters logarithmically or linearly, associated with simple $1/(D-4)$ or $1/(D-3)$ poles respectively. The functions β_{2n} follow straightforwardly from $\mu \frac{d}{d\mu}(1/\mathcal{A}) = 0$ and for C_0 and C_2 can be found from the one-loop graphs in Fig. (6)

$$\beta_0 = \frac{M\mu}{4\pi} C_0^2 \quad , \quad \beta_2 = 2 \frac{M\mu}{4\pi} C_0 C_2 \quad . \quad (21)$$

Integrating these equations relates the C_{2n} coefficients at two different renormalization scales μ and μ_0 . The solution for $C_0(\mu)$ and $C_2(\mu)$ with the boundary condition $C_0(0) = 4\pi a/M$, is

$$C_0(\mu) = \frac{4\pi}{M} \left(\frac{1}{-\mu + 1/a} \right) \quad , \quad C_2(\mu) = C_2(\mu_0) \left(\frac{C_0(\mu)}{C_0(\mu_0)} \right)^2 \quad , \quad (22)$$

which when combined with the boundary condition, $C_2(0) = C_0(0)ar_0/2$, yields $C_2(\mu)$ as given in eq.(19). It is possible to solve the complete, coupled RG equations for the leading small μ behavior of each of the coefficients C_{2n} . The coefficients are

$$C_{2n}(\mu) = \frac{4\pi}{M(-\mu + 1/a)} \left(\frac{r_0/2}{-\mu + 1/a} \right)^n + O(\mu^{-n}) \quad , \quad (23)$$

which has the scaling property in eq.(17). The leading behavior depends on the two parameters a and r_0 encountered when solving for $C_0(\mu)$ and $C_2(\mu)$.

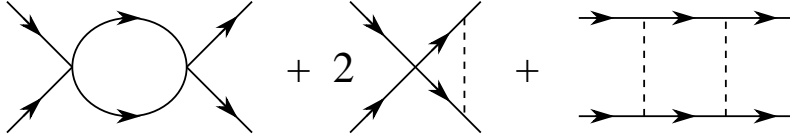


Figure 7: Contributions to the β -functions for C_0 in the theory with pions

This is due to the C_{2n} couplings being driven primarily by lower dimensional interactions.

The inclusion of pions into the theory is straightforward. While the coefficients of the local operators are renormalized, and scale as powers of the renormalization scale μ (we use $Q \equiv \mu \sim p \sim m_q^{1/2}$), the exchange of a single potential pion does not suffer from such renormalizations and therefore pion exchange is a sub-leading contribution, Q^0 . At the same order as the exchange of a potential pion is an insertion of a C_2 operator and a single insertion of the quark mass matrix m_q . Ignoring isospin violation, these operators involving insertions of the light quark mass matrix with coefficients D_2 have the same structure as the C_0 operators. For $\mu \sim m_\pi$, $C_0(\mu) \propto 1/\mu$, $C_2(\mu) \propto 1/\mu^2$ and $D_2(\mu) \propto 1/\mu^2$ for the 1S_0 and 3S_1 channels. A feature of the theory with pions is that this scaling behavior breaks down at low momentum, $p \sim 1/|a|$, and at sufficiently high momentum. The exact beta function for the C_0 coefficients from the graphs in Fig. (7) are

$$\begin{aligned} \beta_0^{(1S_0)} &= \mu \frac{dC_0^{(1S_0)}}{d\mu} = \frac{M\mu}{4\pi} \left\{ \left(C_0^{(1S_0)} \right)^2 + 2C_0^{(1S_0)} \frac{g_A^2}{2f^2} + \left(\frac{g_A^2}{2f^2} \right)^2 \right\} \\ \beta_0^{(3S_1)} &= \mu \frac{dC_0^{(3S_1)}}{d\mu} = \frac{M\mu}{4\pi} \left\{ \left(C_0^{(3S_1)} \right)^2 + 2C_0^{(3S_1)} \frac{g_A^2}{2f^2} + 9 \left(\frac{g_A^2}{2f^2} \right)^2 \right\} \end{aligned} \quad . \quad (24)$$

Solving the RG equation in the 1S_0 channel with the boundary condition $C_0^{(1S_0)}(0) = 4\pi a_1/M$, where a_1 is the 1S_0 scattering length, we find for $\mu \gg 1/|a_1|$

$$C_0^{(1S_0)}(\mu) \simeq -\frac{4\pi}{M\mu} \left(1 + \frac{\mu}{\Lambda_{NN}} \right) , \quad (25)$$

with

$$\Lambda_{NN} = \frac{8\pi f^2}{g_A^2 M} \sim 300 \text{ MeV} , \quad (26)$$

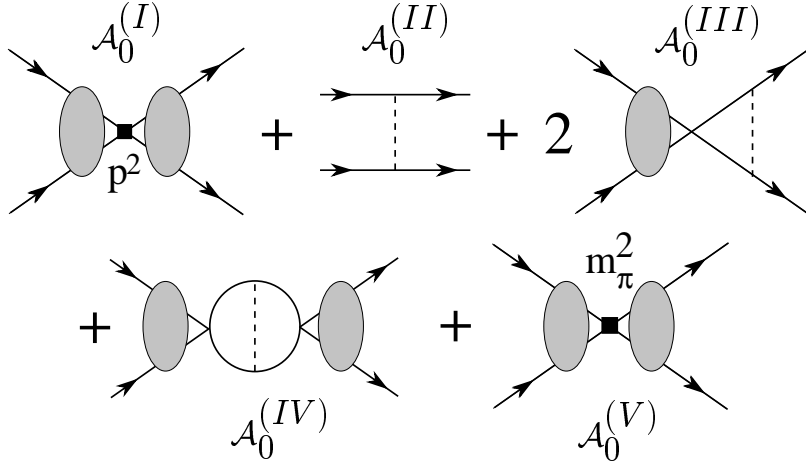


Figure 8: Graphs contributing to the subleading amplitude \mathcal{A}_0 . The shaded ovals are defined in Fig. (5).

and therefore the power counting changes when $\mu \sim \Lambda_{NN}$. The UV fixed point toward which $C_0^{(1S_0)}$ is driven largely cancels the δ -function component of the single potential pion exchange in the 1S_0 channel. As a result, this power counting works only up to $p \sim \Lambda_{NN}$ and the power counting in both channels is expected to fail at momenta on the order of Λ_{NN} . We conclude from this discussion that the expansion parameter for this theory is $\sim m_\pi/\Lambda_{NN} \sim \frac{1}{2}$, which is larger than one would like.

4 NN scattering in the 1S_0 Channel

Having established a consistent power-counting in the previous sections we now apply it to NN scattering in the 1S_0 channel. The amplitude at order Q^{-1} and Q^0 determined from the graphs shown in Fig. (5) and Fig. (8) are

$$\begin{aligned} \mathcal{A}_{-1} &= -\frac{C_0^{(1S_0)}}{1 + C_0^{(1S_0)} \frac{M}{4\pi} (\mu + ip)} , \\ \mathcal{A}_0^{(I)} &= -C_2^{(1S_0)} p^2 \left[\frac{\mathcal{A}_{-1}}{C_0^{(1S_0)}} \right]^2 , \\ \mathcal{A}_0^{(II)} &= \left(\frac{g_A^2}{2f^2} \right) \left(-1 + \frac{m_\pi^2}{4p^2} \ln \left(1 + \frac{4p^2}{m_\pi^2} \right) \right) , \end{aligned}$$

$$\begin{aligned}
\mathcal{A}_0^{(III)} &= \frac{g_A^2}{f^2} \left(\frac{m_\pi M \mathcal{A}_{-1}}{4\pi} \right) \left(-\frac{(\mu + ip)}{m_\pi} + \frac{m_\pi}{2p} X(p, m_\pi) \right) \quad , \\
\mathcal{A}_0^{(IV)} &= \frac{g_A^2}{2f^2} \left(\frac{m_\pi M \mathcal{A}_{-1}}{4\pi} \right)^2 \left(1 - \left(\frac{\mu + ip}{m_\pi} \right)^2 + iX(p, m_\pi) - \ln \left(\frac{m_\pi}{\mu} \right) \right) \quad , \\
\mathcal{A}_0^{(V)} &= -D_2^{(1S_0)} m_\pi^2 \left[\frac{\mathcal{A}_{-1}}{C_0^{(1S_0)}} \right]^2 \quad , \\
X(p, m_\pi) &= \tan^{-1} \left(\frac{2p}{m_\pi} \right) + \frac{i}{2} \ln \left(1 + \frac{4p^2}{m_\pi^2} \right) \quad . \tag{27}
\end{aligned}$$

At order Q^{-1} there is one unknown coefficient $C_0^{(1S_0)}$ that must be determined from data while at order Q^0 there are three unknown coefficients $C_0^{(1S_0)}, C_2^{(1S_0)}$ and $D_2^{(1S_0)}$ that must be determined. The graph giving $\mathcal{A}_0^{(IV)}$ is divergent in four dimensions and therefore gives rise to the logarithmic dependence on the renormalization scale μ in eq. (27) (we have performed a finite subtraction, in addition to the usual *PDS*). In order for the expansion to converge, the leading term \mathcal{A}_{-1} must capture most of the scattering length, and hence the subtraction. For this scattering channel we examine the phase shift δ , and perform a perturbative expansion of δ in Q , $\delta = \delta^{(0)} + \delta^{(1)} + \dots$. It is straightforward to relate the phase shift to the amplitude,

$$\begin{aligned}
\delta &= \frac{1}{2i} \ln \left(1 + i \frac{Mp}{2\pi} \mathcal{A} \right) \quad , \\
\delta^{(0)} &= \frac{1}{2i} \ln \left(1 + i \frac{Mp}{2\pi} \mathcal{A}_{-1} \right) \quad , \quad \delta^{(1)} = \frac{Mp}{4\pi} \left(\frac{\mathcal{A}_0}{1 + i \frac{Mp}{2\pi} \mathcal{A}_{-1}} \right) \quad . \tag{28}
\end{aligned}$$

There are several ways to determine the coefficients from observables. One fit we have performed is to the results of the Nijmegen partial-wave analysis²¹ over a momentum range $p \leq 200$ MeV, from which we find for $\mu = m_\pi$

$$C_0^{(1S_0)} = -3.34 \text{ fm}^2 \quad , \quad D_2^{(1S_0)} = -0.42 \text{ fm}^4 \quad , \quad C_2^{(1S_0)} = 3.24 \text{ fm}^4 \quad , \tag{29}$$

giving the dashed curve plotted in Fig. (9). Fitting the scattering length and effective range gives (requiring $D_2(m_\pi) = 0$), for $\mu = m_\pi$

$$C_0 = -3.63 \text{ fm}^2 \quad , \quad C_2 = 2.92 \text{ fm}^4 \quad , \tag{30}$$

and the dotted curve in Fig. (9). It is clear from Fig. (9) that the corrections to the leading order result become substantial above ~ 200 MeV and we expect the expansion to become unreliable at momenta larger than this value.

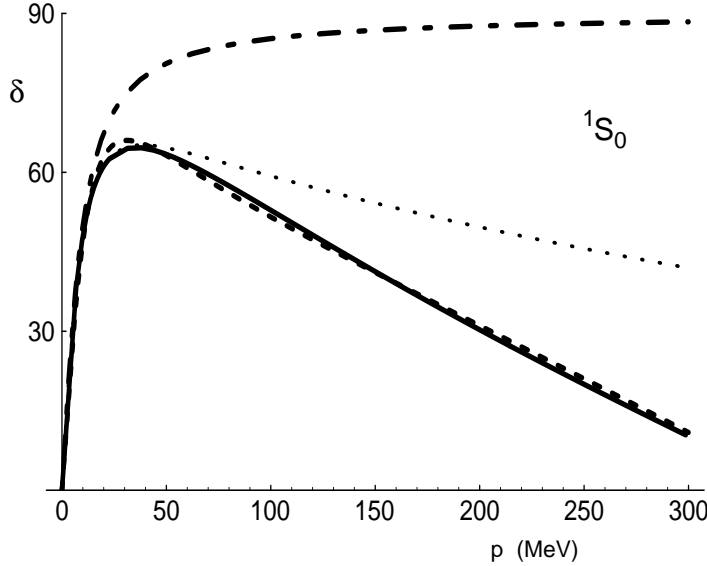


Figure 9: The phase shift δ for the 1S_0 channel. The dot-dashed curve is the one parameter fit at order Q^{-1} , that reproduces the scattering length. The dashed curve corresponds to fitting δ between $0 < p < 200$ MeV, while the dotted curve corresponds to fitting the scattering length and effective range. The solid line shows the results of the Nijmegen partial wave analysis.

We chose to renormalize at $\mu = m_\pi$ for our numerical analysis, but as the amplitudes are explicitly μ -independent we could have chosen any value of μ , with $\Lambda_{NN} \gg \mu \gg 1/a$. The logarithm appearing in the subleading amplitude suggests we choose $\mu \sim m_\pi$.

5 NN scattering in the $^3S_1 - ^3D_1$ Channel

The analysis of scattering in the $^3S_1 - ^3D_1$ channel is a straightforward extension of the analysis performed in the 1S_0 channel. The important difference is that the nucleons in the initial and final states with total angular momentum $J = 1$ can be in an orbital angular momentum state of either $L = 0$ or $L = 2$. The power counting for amplitudes that take the nucleons from a 3S_1 -state to a 3S_1 -state is identical to the analysis in the 1S_0 -channel. In fact, the expression for these amplitudes are exactly the same with the appropriate substitution of coefficients. Operators between two 3D_1 states are not renormalized by the leading operators, which project out only 3S_1 states. Further, they involve a

total of four spatial derivatives, two on the incoming nucleons, and two on the out-going nucleons. Therefore, such operators contribute at order Q^3 , and can be neglected. Consequently, amplitudes for scattering from an 3D_1 state into an 3D_1 state are dominated by single potential pion exchange which contributes at order Q^0 . Operators connecting 3D_1 and 3S_1 states involve 2 spatial derivatives (acting on the 3D_1 state) and are renormalized by the leading operators, but only on the $L = 0$ “side” of the operator. Therefore the coefficient of this operator, $C_2^{({}^3S_1-{}^3D_1)} \sim 1/\mu$, contributing at order Q^1 and it can be neglected at order Q^0 . Thus, mixing between 3D_1 and 3S_1 states is dominated by single potential pion exchange dressed by a bubble chain of $C_0^{({}^3S_1)}$ operators and a parameter free prediction for this mixing exists at order Q^0 .

We denote the amplitude at order Q^n by $\mathcal{A}_{n[LL']}$, where L and L' are the initial and final orbital angular momenta. At leading order Q^{-1} in the expansion there is a contribution only to the 3S_1 partial wave:

$$\mathcal{A}_{-1[00]} = -\frac{C_0^{({}^3S_1)}}{1 + C_0^{({}^3S_1)} \frac{M}{4\pi} (\mu + ip)} , \quad \mathcal{A}_{-1[02]} = \mathcal{A}_{-1[20]} = \mathcal{A}_{-1[22]} = 0 \quad (31)$$

At order Q^0 there are contributions from graphs of the same form as in the amplitude for 1S_0 scattering, shown in Fig. (8). Using the same identification of graphs as in the 1S_0 channel, $\mathcal{A}_{0[L,L']} = \mathcal{A}_{0[L,L']}^{(I)} + \dots$, we find that

$$\begin{aligned} \mathcal{A}_{0[00]}^{(I)} &= -C_2^{({}^3S_1)} p^2 \left[\frac{\mathcal{A}_{-1[00]}}{C_0^{({}^3S_1)}} \right]^2 , \quad \mathcal{A}_{0[02]}^{(I)} = \mathcal{A}_{0[20]}^{(I)} = \mathcal{A}_{0[22]}^{(I)} = 0 , \\ \mathcal{A}_{0[00]}^{(II)} &= -\frac{g_A^2}{2f^2} \left[1 - \frac{m_\pi^2}{2p^2} Q_0(z) \right] , \\ \mathcal{A}_{0[02]}^{(II)} &= \mathcal{A}_{0[20]}^{(II)} = -\frac{g_A^2}{\sqrt{2}f^2} [Q_0(z) + Q_2(z) - 2Q_1(z)] , \\ \mathcal{A}_{0[22]}^{(II)} &= -\frac{g_A^2 m_\pi^2}{4f^2 p^2} \left[Q_2(z) + \frac{6p^2}{5m_\pi^2} (Q_1(z) - Q_3(z)) \right] , \\ \mathcal{A}_{0[00]}^{(III)} &= \frac{g_A^2}{f^2} \left(\frac{m_\pi M \mathcal{A}_{-1[00]}}{4\pi} \right) \left(-\frac{(\mu + ip)}{m_\pi} + \frac{m_\pi}{2p} X(p, m_\pi) \right) , \\ \mathcal{A}_{0[02]}^{(III)} &= \mathcal{A}_{0[20]}^{(III)} \\ &= \frac{g_A^2}{\sqrt{2}f^2} \left(\frac{M \mathcal{A}_{-1[00]}}{4\pi} \right) p^2 \left[-\frac{3m_\pi^3}{4p^4} + \frac{m_\pi^2}{8p^5} (3m_\pi^2 + 4p^2) \tan^{-1} \left(\frac{2p}{m_\pi} \right) \right] \end{aligned}$$

$$\begin{aligned}
& + i \left(-\frac{3m_\pi^2}{4p^3} + \frac{1}{2p} + \frac{m_\pi^2}{4p^3} \left(1 + \frac{3m_\pi^2}{4p^2} \right) \log \left(1 + \frac{4p^2}{m_\pi^2} \right) \right) \Big] \quad , \\
\mathcal{A}_{0[22]}^{(III)} &= 0 \quad , \\
\mathcal{A}_{0[00]}^{(IV)} &= \frac{g_A^2}{2f^2} \left(\frac{m_\pi M \mathcal{A}_{-1[00]}}{4\pi} \right)^2 \left(1 - \left(\frac{\mu + ip}{m_\pi} \right)^2 + iX(p, m_\pi) - \ln \left(\frac{m_\pi}{\mu} \right) \right) \quad , \\
\mathcal{A}_{0[02]}^{(IV)} &= \mathcal{A}_{0[20]}^{(IV)} = \mathcal{A}_{0[22]}^{(IV)} = 0 \quad , \\
\mathcal{A}_{0[00]}^{(V)} &= -D_2^{(3S_1)} m_\pi^2 \left[\frac{\mathcal{A}_{-1[00]}}{C_0^{(3S_1)}} \right]^2 \quad , \quad \mathcal{A}_{0[02]}^{(V)} = \mathcal{A}_{0[20]}^{(V)} = \mathcal{A}_{0[22]}^{(V)} = 0 \quad (32)
\end{aligned}$$

where $z = 1 + m_\pi^2/(2p^2)$ and $Q_k(z)$ denotes the k -th order irregular Legendre function. Again part of the subtraction point independent contribution to $\mathcal{A}_{0[00]}^{(IV)}$ has been absorbed into $\mathcal{A}_{0[00]}^{(V)}$. The S-matrix in this channel is expressed in terms of two phase shifts, δ_0 and δ_2 , and a mixing angle ε_1 ,

$$S = 1 + i \frac{pM}{2\pi} \mathcal{A} = \begin{pmatrix} e^{2i\delta_0} \cos 2\varepsilon_1 & ie^{i(\delta_0 + \delta_2)} \sin 2\varepsilon_1 \\ ie^{i(\delta_0 + \delta_2)} \sin 2\varepsilon_1 & e^{2i\delta_2} \cos 2\varepsilon_1 \end{pmatrix} \quad , \quad (33)$$

and like the 1S_0 channel we will expand S order by order in Q .

As the $^3S_1 - ^3D_1$ mixing parameter has vanishing contribution at order Q^0 it starts at order Q^1 , the same holds true for δ_2 . Writing each of the parameters as an expansion in Q ,

$$\delta_0 = \delta_0^{(0)} + \delta_0^{(1)} + \dots, \quad \delta_2 = \delta_2^{(0)} + \delta_2^{(1)} + \dots, \quad \varepsilon_1 = \varepsilon_1^{(0)} + \varepsilon_1^{(1)} + \dots, \quad (34)$$

it follows that

$$\delta_0^{(0)} = -\frac{i}{2} \log \left[1 + i \frac{pM}{2\pi} \mathcal{A}_{-1[00]} \right] \quad , \quad \delta_0^{(1)} = \frac{pM}{4\pi} \frac{\mathcal{A}_{0[00]}}{1 + i \frac{pM}{2\pi} \mathcal{A}_{-1[00]}} \quad , \quad (35)$$

$$\varepsilon_1^{(0)} = 0 \quad , \quad \varepsilon_1^{(1)} = \frac{pM}{4\pi} \frac{\mathcal{A}_{0[02]}}{\sqrt{1 + i \frac{pM}{2\pi} \mathcal{A}_{-1[00]}}} \quad , \quad (36)$$

$$\delta_2^{(0)} = 0 \quad , \quad \delta_2^{(1)} = \frac{pM}{4\pi} \mathcal{A}_{0[22]} \quad . \quad (37)$$

Fitting the parameters $C_0^{(3S_1)}$, $C_2^{(3S_1)}$ and $D_2^{(3S_1)}$ to the phase shift δ_0 over the

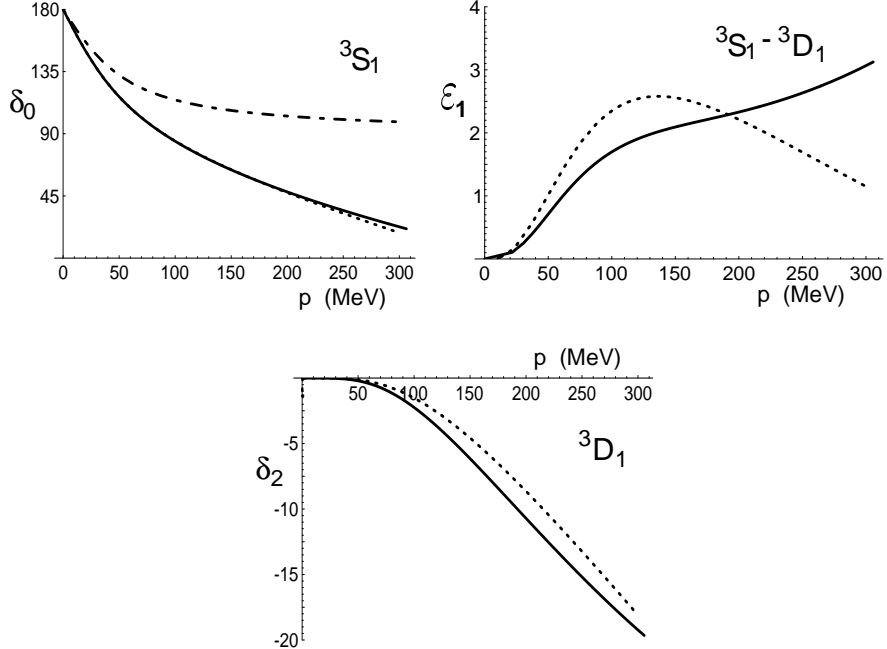


Figure 10: The phase shifts δ_0 , δ_2 and mixing parameter ε_1 for the $^3S_1 - ^3D_1$ channel. The solid line denotes the results of the Nijmegen partial wave analysis. The dot-dashed curve is the fit at order Q^{-1} for δ_0 , while $\delta_2 = \varepsilon_1 = 0$ at this order. The dashed curves are the results of the order Q^0 fit of δ_0 to the partial wave analysis over the momentum range $p \leq 200$ MeV.

momentum range $p \leq 200$ MeV yields, at $\mu = m_\pi$

$$C_0^{(^3S_1)} = -5.51 \text{ fm}^2, \quad D_2^{(^3S_1)} = 1.32 \text{ fm}^4, \quad C_2^{(^3S_1)} = 9.91 \text{ fm}^4. \quad (38)$$

The dashed curves in Fig. (10) show the phase shifts δ_0 , δ_2 and mixing parameter ε_1 compared to the Nijmegen partial wave analysis²¹ for this set of coefficients. There are no free parameters at this order in either ε_1 or δ_2 once $C_0^{(^3S_1)}$ has been determined from δ_0 .

6 Higher Order Effects

A local operator that connects an orbital angular momentum L state with an orbital angular momentum L' state involves at least $L + L'$ spatial derivatives.

If either L or L' but not both correspond to an S -wave then the operator enters at order $Q^{L+L'-1}$. However, if neither L nor L' correspond to an S -wave then the operator contributes at order $Q^{L+L'}$ when L, L' is odd and at order $Q^{L+L'-1}$ when L, L' is even. The contribution of pions is at order Q^0 , and is therefore the leading contribution to all non S -wave to S -wave scattering amplitudes.

Implicit in all previous discussions we have been retaining only the contribution to diagrams from the nucleon poles. While these are the leading contribution by factors of the nucleon mass, there are higher order contributions arising from other poles, when present. The leading contribution from the pion radiation regime (hence the term radiation pions, in analogy with the terminology in non-relativistic gauge theories^{22–26}) does not contribute to the β -functions of the $C_0(\mu)$ due to the explicit factors of m_π but to the β -functions of the $D_2(\mu)$. Further, such contributions give rise to mixing between the operators in the 1S_0 and 3S_1 channels,

$$\begin{aligned}\beta_{D_2^{(1S_0)}}^{(rad)} &= + \frac{3g_A^2}{4\pi^2 f^2} \left(C_0^{(3S_1)} - C_0^{(1S_0)} \right) \quad , \\ \beta_{D_2^{(3S_1)}}^{(rad)} &= - \frac{3g_A^2}{4\pi^2 f^2} \left(C_0^{(3S_1)} - C_0^{(1S_0)} \right) .\end{aligned}\quad (39)$$

A comment on the role of baryonic resonances is appropriate. The impact of the Δ resonance has been determined with Weinberg's power-counting in two different prescriptions^{2,9} ^d. It is found not to play an important role in NN scattering as the mass scale that sets the size of its contribution is $\sqrt{M(M_\Delta - M)} \sim 500$ MeV. This scale is higher than the scale at which the theory breaks down, Λ_{NN} , and so it is appropriate not to include the baryonic resonances, until the theory above the scale Λ_{NN} is constructed.

7 Conclusions

After several years of investigation we now understand the limitations of Weinberg's power-counting¹. In theories with large scattering lengths as arise in NN scattering in the 1S_0 and $^3S_1 - ^3D_1$ channels, simply counting derivatives or number of insertions of the light quark mass matrix does not correspond directly to the degree of suppression of an operator. A new power-counting scheme has been introduced¹⁷ which allows simple identification of graphs that contribute at a given order. In the new power-counting scheme pions are

^dThe $\Delta(1232)$ and other baryon resonances have been consistently included in the single nucleon sector²⁷.

sub-leading compared to the leading local four-nucleon operators and can be treated in perturbation theory. The regulation problems found in Weinberg's theory do not arise. Explicit computation of NN scattering in the 1S_0 and $^3S_1 - ^3D_1$ channels to sub-leading order has been presented. Most impressive perhaps is the parameter-free prediction of the $^3S_1 - ^3D_1$ mixing parameter ε_1 which agrees well with the Nijmegen phase shift analysis.

The future looks extremely promising for a systematic effective field theory analysis of nuclear physics. The short term program will be to examine the two-body systems in detail, i.e. the properties of the deuteron²⁸ and inelastic processes. In the long-term one hopes to make progress in many-body systems. Some impressive results have already been obtained¹⁴ in the three-body systems.

I would like to thank my co-organizers of this meeting, Ryoichi Seki and Bira van Kolck, who did all the hard work and who convinced El Nino to stay away. I would also like to thank my collaborators, David Kaplan and Mark Wise. This work is supported in part by Department of Energy Grant DE-FG03-97ER41014.

References

1. S. Weinberg, *Phys. Lett. B* **251**, 288 (1990); *Nucl. Phys. B* **363**, 3 (1991); *Phys. Lett. B* **295**, 114 (1992).
2. C. Ordonez and U. van Kolck, *Phys. Lett. B* **291**, 459 (1992); C. Ordonez, L. Ray and U. van Kolck, *Phys. Rev. Lett.* **72**, 1982 (1994) ; *Phys. Rev. C* **53**, 2086 (1996) ; U. van Kolck, *Phys. Rev. C* **49**, 2932 (1994) .
3. T.S. Park, D.P. Min and M. Rho, *Phys. Rev. Lett.* **74**, 4153 (1995) ; *Nucl. Phys. A* **596**, 515 (1996).
4. D.B. Kaplan, M.J. Savage and M.B. Wise, *Nucl. Phys. B* **478**, 629 (1996), nucl-th/9605002.
5. T. Cohen, J.L. Friar, G.A. Miller and U. van Kolck, *Phys. Rev. C* **53**, 2661 (1996).
6. D. B. Kaplan, *Nucl. Phys. B* **494**, 471 (1997).
7. T.D. Cohen, *Phys. Rev. C* **55**, 67 (1997). D.R. Phillips and T.D. Cohen, *Phys. Lett. B* **390**, 7 (1997). K.A. Scaldeferri, D.R. Phillips, C.W. Kao and T.D. Cohen, *Phys. Rev. C* **56**, 679 (1997). S.R. Beane, T.D. Cohen and D.R. Phillips, nucl-th/9709062.
8. J.L. Friar, Few Body Syst. **99**, 1 (1996), nucl-th/9607020.
9. M.J. Savage, *Phys. Rev. C* **55**, 2185 (1997), nucl-th/9611022.

10. M. Luke and A.V. Manohar, *Phys. Rev. D* **55**, 4129 (1997), [hep-ph/9610534](#) .
11. G.P. Lepage, [nucl-th/9706029](#), Lectures given at 9th Jorge Andre Swieca Summer School: Particles and Fields, Sao Paulo, Brazil, 16-28 Feb 1997.
12. S.K. Adhikari and A. Ghosh, *J. Phys. A* **30**, 6553 (1997).
13. K.G. Richardson, M.C. Birse and J.A. McGovern, [hep-ph/9708435](#).
14. P.F. Bedaque and U. van Kolck, [nucl-th/9710073](#); P.F. Bedaque, H.-W. Hammer and U. van Kolck, [nucl-th/9802057](#).
15. U. van Kolck, Talk given at Workshop on Chiral Dynamics: Theory and Experiment (ChPT 97), Mainz, Germany, 1-5 Sep 1997. [hep-ph/9711222](#)
16. T.S. Park, K. Kubodera, D.P. Min and M. Rho, [hep-ph/9711463](#).
17. D.B. Kaplan, M.J. Savage and M.B. Wise, [nucl-th/9801034](#), *to appear in Phys. Lett. B*; [nucl-th/9802075](#), *submitted to Nucl. Phys. B*.
18. J. Gegelia, [nucl-th/9802038](#).
19. J.V. Steele and R.J. Furnstahl, [nucl-th/9802069](#).
20. A. Manohar and H. Georgi, *Nucl. Phys. B* **234**, 189 (1984).
21. V.G.J. Stoks, R.A.M. Klomp, C.P.F. Terheggen and J.J. de Swart, *Phys. Rev. C* **49**, 2950 (1994), [nucl-th/9406039](#).
22. M. Luke and A.V. Manohar, *Phys. Lett. B* **286**, 348 (1992), [hep-ph/9205228](#).
23. P. Labelle, [hep-ph/9608491](#).
24. B. Grinstein and I.Z. Rothstein, *Phys. Rev. D* **57**, 78 (1998). [hep-ph/9703298](#).
25. M. Luke and M.J. Savage, *Phys. Rev. D* **57**, 413 (1998), [hep-ph/9707313](#).
26. H. Griesshammer, [hep-ph/9712467](#).
27. E. Jenkins and A.V. Manohar, talk presented at the Workshop on Effective Field Theories of the Standard Model, Dobogoko, Hungary, Aug 1991. Published in *Effective Field Theories of the Standard Model*, ed. U. Meissner, World Scientific, Singapore (1992).
28. D.B. Kaplan, M.J. Savage and M.B. Wise, [nucl-th/9804032](#).